Subproject A2.8

Optical Microcavities

Principle Investigators: Heinz Kalt and Michael Hetterich

CFN-Financed Scientists:

Further Scientists: Daniel Rülke, Frank Michael Weber, Torsten Beck, Philipp Burger, Florian Stockmar, Christoph Reinheimer, Benoit Ramadout, Fabian Pérez-Willard, Dr. Erich Müller, Peter Pfundstein, Jacques Hawecker, PD Dr. Frank Schmidt (Konrad-Zuse-Zentrum für Informationstechnik Berlin, ZIB), Dr. Sven Burger (ZIB), Benjamin Kettner (ZIB)

Institut für Angewandte Physik
Karlsruhe Institute of Technology (KIT)

Optical Microcavities

Introduction and Overview

The aim of A2.8 is to develop and investigate optical microcavity structures and devices within the context of possible applications in quantum optics (such as single photon sources) and quantum information processing. Our approach to realize the latter is based on electronic/excitonic (spin) states in quantum dots (QDs) as quantum bits (qubits). QDs – in particular the InGaAs/GaAs dots used within A2 – have been identified as promising candidates for quantum information storage due to their long spin life and coherence times for electrons and even excitons, both in the literature and our own work (see A2.3). To initialize spin states in QDs and read them out optically, single-QD spin-injection light-emitting diodes (spin-LEDs) with the highest injection efficiency worldwide (close to 100%) have been developed together with A2.3 (as well as first transistor structures for controlled hole injection, see corresponding report). Very recently we could also demonstrate that these devices can be utilized as electrically pumped emitters for single spin-polarized photons with the highest polarization degree achieved so far (see Sect.3). Such devices might be interesting for secure data transmission via fast fiber-optic networks.

To realize quantum-logical *operations* between spin-qubits, a controllable and *coherent coupling* of spin states stored in spatially separated QDs is needed. As discussed in Sect.1, we aim to realize such an interaction via the light field by inserting the dots in properly designed (*connected) optical cavities*, an approach first suggested by *Imamoğlu et al.* [1], which – however – has not been realized experimentally so far in the literature. Nevertheless, the feasibility of this approach is supported by a number of results, e.g., the demonstration of pillar cavity quality factors *Q* exceeding 150000, as well as the observation of strong coupling of a cavity mode with a *single* dot [2] and electro-optical tuning of the QD energy to control the coupling with the light field [3].

To realize an optical coupling between spatially separated dots, but also for other quantum-optical applications like single photon sources, we develop standard (coupled) pillar cavities (Sect.1) as well as novel pyramidal resonators (Sect.2). These have already attracted strong interest both in the scientific community (e.g., in Nature Photonics [A2.8:5]) as well as the public (e.g., contributions to a nanotechnology exhibition by the *Technoseum* Mannheim, Germany, in 2010, to the textbook by P.A. Tipler and G. Mosca: *Physik für Wissenschaftler und Ingenieure*, Spektrum Akademischer Verlag, 2009, as well as reports in the media (e.g., *Frankfurter Allgemeine Zeitung* and *Radio Regenbogen* [4]). Electric fields applied to the cavities shall be used to tune the QD emission wavelength in and out of the cavity modes and control the QD coupling. As discussed in Sect.3 a pyramidal shape is advantageous for quantum-optical applications since it easily enables structures with few or even single dots by introducing the QD layer close to the pyramid tip. Furthermore, the pyramid facets can be coated by distributed Bragg reflectors (DBRs) in order to suppress leaky modes and achieve a true three-dimensional confinement. Having demonstrated the feasibility of this approach [5] we currently develop contacted pyramidal resonators with few QDs in order to realize an electrically pumped single photon source (see Sect.3). Furthermore, we closely cooperate with the young scientist group of *D. Schaadt* (A2.6) with the aim to achieve QD positioning in our cavities. Recently, we have also extended our studies to the investigation of the high-*Q* cavities realized in A5.4, which shall be one of the core research topics in the next funding period.

1. Single and Coupled Pillar-Type Cavities

The pillar-type resonators studied in this subproject [A2.8:7,A2.8:9,A2.8:15,6,7,8] consist of a one-wavelength thick GaAs cavity with embedded InGaAs quantum dots as internal broad-band light source (emission wavelength ~950 nm), surrounded by top and bottom AlAs / GaAs DBRs (typically 20–25 pairs). The planar layer structures were grown by molecular-beam epitaxy in close collaboration between A2.8 and A2.6 (*D. Schaadt*). To process the actual resonators we used the focused ion beam (FIB) facility of the Nanostructure Service Laboratory. The structural assessment by electron microscopy was done in cooperation with A2.5 (*D. Gerthsen*). Examples for the cavities obtained are shown in Fig. 1.

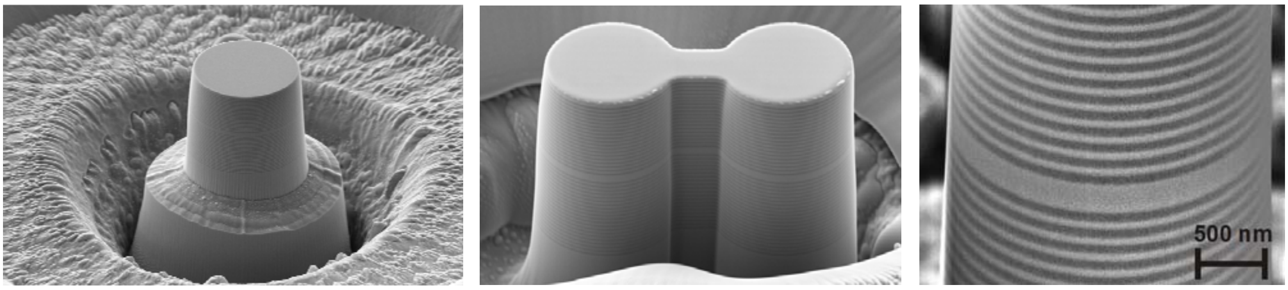

Fig.1: Scanning electron microscopy (SEM) images of processed pillar cavities. Left: single pillar (diameter: 7 µm), middle: coupled pillar structure (diameter: 4.8 µm, bridge width: 1.8 µm, center distance: 6 µm) [A2.8:9], right: magnified cavity region of optimized structure.

Our optimized FIB procedure starts with rough milling using a high ion current. Then the latter is reduced in three steps from 5 nA down to 50–100 pA for final polishing [A2.8:7]. Utilizing a recently established improved point-wise FIB milling process, structures with extremely smooth sidewalls, i.e., no detectable surface roughness in scanning electron micrographs can be obtained. In this way, single pillars with diameters from 0.9–15 µm as well as the coupled structures discussed below could be realized. Figure 2 shows the different steps of the fabrication process.

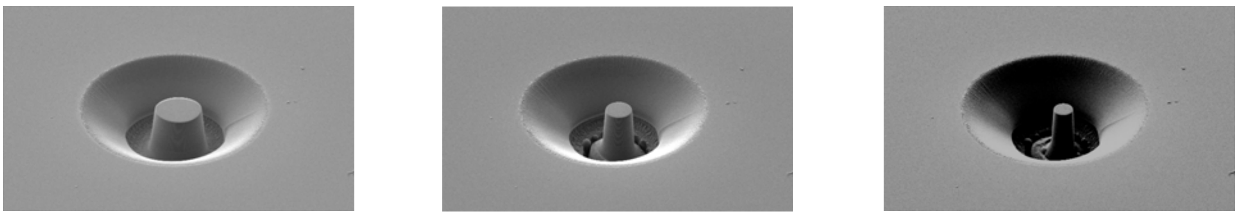

after 5 nA ion current | *after 500 pA ion current* | *after 50 –100 pA ion current*

Fig.2: FIB milling of pillar microcavities. SEM images of different process steps.

To study the optical modes in the processed microcavities, a confocal micro-photoluminescence (µ-PL) set-up with a variable temperature cryostat was used. As an example, the inset of Fig.4 shows the measured mode spectrum of a single 5.5 µm pillar resonator. For the cavity design studies discussed below, were the quality factor was not the main concern, typical Q factors ranged from about 9000 for a pillar diameter of d = 3 µm to 18000 for d = 5 µm. Among other factors, these values were partly limited by the number of Bragg pairs used (2 x 25). However, since quantum-optical applications will require optimal light confinement in the future we recently put increased effort in further optimization of the fabrication procedure. To this end we increased the number of Bragg pairs to 32 (top) / up to 40 (bottom) and improved the FIB milling process conditions.

Furthermore, growth was interrupted after deposition of the bottom DBR in order to optically characterize it and adapt the growth rates for the top DBR accordingly. Thus the influence of growth rate instabilities could be minimized. As a result, *Q* improved by ~30% to maximum values of ~40000 for large pillars, sufficient for the applications targeted in the current funding period. These values are now limited by the fabrication process itself, i.e., background absorption at the pillar sidewalls due to FIB induced damage and the remaining growth rate instabilities of the used MBE system. Therefore, a further improvement would require additional investments (in particular new more stable Al / As sources), a route which, however, will not be pursued further, since the main focus will shift to a different resonator type in the next funding period (see Sect.4) and MBE will no longer be available then (leave of *D. Schaadt*).

Theoretical Modeling

While pillar cavities are commonly used for quantum-optical experiments and strong coupling of a single QD state with a pillar cavity mode has been demonstrated [2], the theoretical potential of this resonator type (e.g., maximum *Q* for realistic conditions) has surprisingly not been explored thoroughly enough in the literature so far. In a joint effort with the *DFG Research Center MATHEON Berlin (F. Schmidt, S. Burger)* we therefore performed detailed and accurate numerical studies based on Finite Element Methods (FEM) concerning the influence of different structural parameters (pillar diameter, number of Bragg pairs, side wall inclination angle, bottom DBR etched through or not, etc.) on the optical cavity modes and *Q* factors for *realistic material parameters*, in particular taking into account background absorption in GaAs, i.e., the finite imaginary part of its permittivity [A2.8:15]. The results showed good agreement with experimental data. As an example for the calculations performed, Fig.3a depicts theoretical *Q* factors for micro-pillars with a diameter of 3.3 µm, when the number of top and bottom DBR pairs is varied simultaneously.

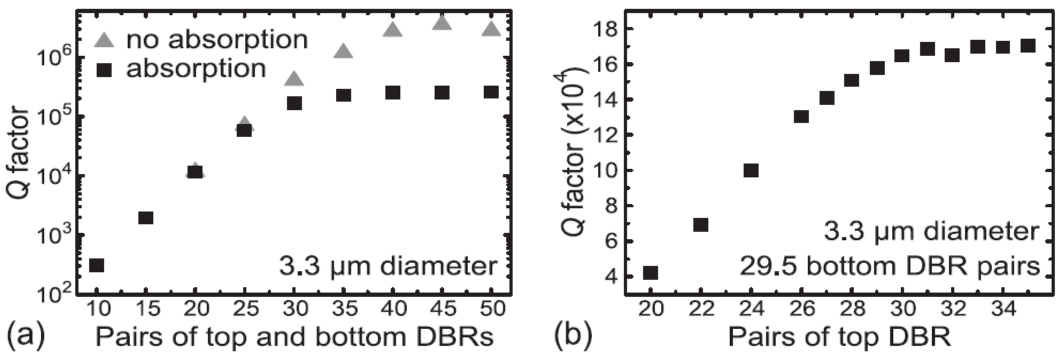

Fig.3: *Q* factors for micro-pillars with a diameter of 3.3 µm. (a) Variation of top and bottom DBR pairs simultaneously with or without absorption in the cavity material (GaAs). (b) Variation of top DBR pairs with fixed number of bottom DBR pairs. Taken from [A2.8:15].

As can clearly be seen, the DBR reflectivity (number of Bragg pairs) limits the *Q* factor for up to 25 pairs, however, for ultrahigh-*Q* (~100000 or more) cavities, requiring 30 or more pairs, GaAs background absorption finally limits the quality factor which saturates in this case at around 168000 (Fig.3b). It is important to note, that the theoretical limits resulting from our calculations (the absolute maximum is *Q* ~ 250000 for > 40 DBR pairs) are already approached by existing "world record" pillar cavities with similar parameters [9]. On the one hand this demonstrates the usefulness of our calculations, however, on the other hand it also gives clear evidence, that these structures are already optimized to such an extent, that their theoretical potential is nearly fully exploited, i.e., there is not much room for further improvement. Therefore, details of the structural design become very important. For instance, we could show that the cavity Q is a non-monotonous function of the pillar diameter and the sidewall inclination angle [A2.8:15] which means that a careful optimization is required for optimum results.

In order to enable us to model Bragg cavities with *arbitrary lateral shape* and design their mode properties according to our requirements, we implemented a simple but versatile numerical simulation technique. In the latter, the resonator is essentially treated as a step-index waveguide with ideal end mirrors, and the lateral field distribution is again calculated using a Finite Element Method [A2.8:7,A2.8:9]. As a test we applied our model to single cylindrical resonators and compared the found resonances with our experimental results for pillars with different diameters. As can be seen in Fig.4, excellent agreement could be achieved, which clearly indicated that our simplified approach should be sufficiently accurate to design more complex resonator geometries.

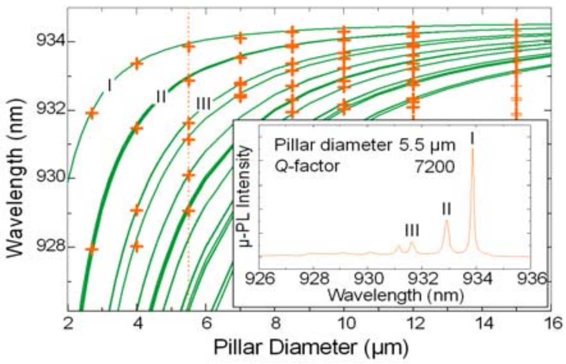

Fig.4: Simulated (solid lines) and experimentally found (crosses) resonance wavelengths in single pillar cavities as a function of their diameter. The inset shows a typical µ-PL spectrum [A2.8:7].

Connected Pillar Cavities

For the future realization of an optically mediated coupling between spatially separated quantum dot states, *connected* resonators (i.e., photonic “molecules”) have been investigated. In such structures, individual cavities (ideally containing only a single suitably positioned dot each) could be selectively addressed via appropriate *localized* modes (e.g., for *read-out* processes), while *delocalized* modes would be used to *couple* QDs in different cavities. To this end we have developed *unsymmetrical connected micropillar cavities* [A2.8:7,A2.8:9,6,7], extending previous work of *Bayer et al.* [10]. An example is shown in Fig.5. Utilizing the numerical tools mentioned above, the latter have been designed in such a way, that both modes *localized* in either of the pillars as well as *delocalized* modes should coexist in the same structure. Figure 6 (top) shows the calculated intensity distributions of the three lowest modes in a properly designed connected double cavity. Indeed, the first two modes are localized, while the third mode has a delocalized character.

To verify this coexistence of different mode types experimentally, spatially resolved µ-PL measurements have been carried out. The results are shown in the bottom part of Fig.6. As can be seen, the spectral positions of the different modes obtained from our theoretical model (vertical lines in the spatially integrated spectra) agree excellently with experiment. In order to investigate if the latter possess a localized or delocalized character, the µ-PL measurements have been carried out with excitation of only one of the two connected pillars (the wider in the upper and the smaller in the lower image shown in Fig.6). It is found that for the *delocalized* mode the intensity distribution is spread over the whole photonic structure, as predicted. Furthermore, the distribution essentially looks the same, no matter where excitation takes place. That means the QDs in both pillars interact equally well with that mode, i.e., the latter should be suitable for optically coupling dot states in the connected cavities. The *localized* modes on the other hand are always confined to either of the pillars. That means they could indeed be utilized to read out quantum dot states in one part of the photonic structure without disturbing the other.

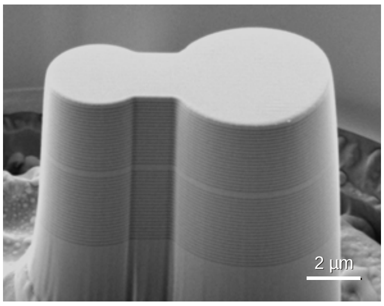

Fig.5: Unsymmetrical coupled pillar micro-cavity.

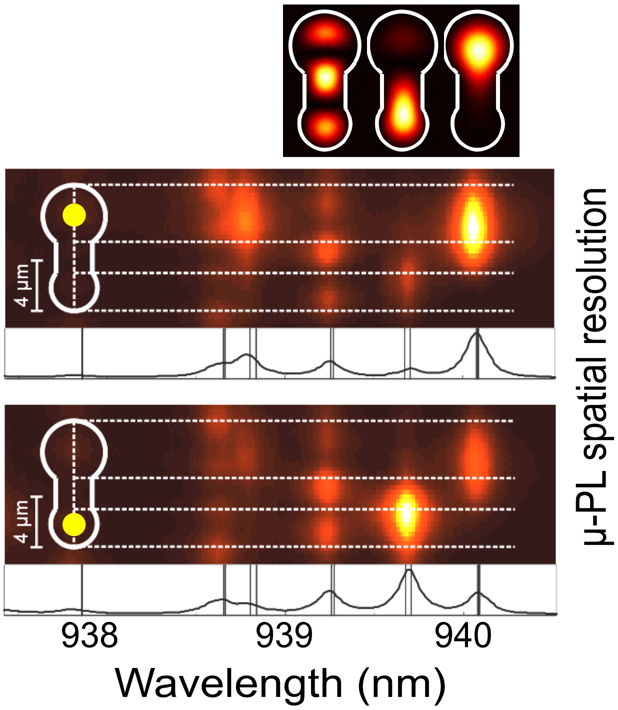

Fig.6: Top: Calculated color-coded intensity distribution of the lowest three optical modes in a coupled pillar structure with pillar diameters of 5.0 µm and 3.7 µm, a center distance of 5.7 µm, and a bridge width of 2.9 µm. Bottom: Spatially resolved color-coded µ-PL spectra of the same structure. The contour on the left indicates the detection positions by a vertical dashed line as well as the position in the spatial resolution. The spectra below the images display the spatially integrated µ-PL intensity and the resonance wavelengths obtained from our theoretical model (vertical lines). The results of two measurements are shown, which only differ in the excitation position. The latter was chosen to be on the wider pillar in the upper and on the smaller pillar in the lower case.

Electrical Tuning of Quantum Dot States

As the next step we have started to develop devices that enable an electrical *tuning* of single QD emission lines in and out of resonance with the different cavity modes to actively control their coupling. Examples for such structures, where an electric field is applied vertically (left) or laterally (right), respectively, are shown in Fig.7.

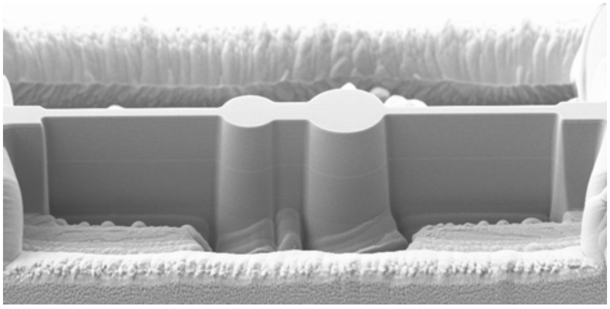

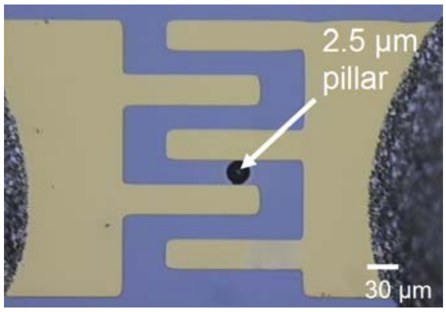

Fig.7: Left: Contacted coupled pillar cavity with doped DBRs used to apply vertical electric fields to the embedded QDs. Right: Pillar cavity surrounded by interdigitated gold electrodes to apply lateral fields.

Since the applied voltages can lead so significant photocurrents and thus heating of the structures, AC fields have been used to distinguish the true Quantum-Confined Stark effect (QCSE) from the thermal shift of the QD emission wavelength. (The latter is often dominant, which has obviously been overlooked in some reports in the literature.) Typical QCSE-related shifts of ~0.06 nm/V have been obtained, which should be sufficient to control the coupling of a QD state with an optical mode. It should be noted that the same approach can also be used to suppress the exciton fine structure splitting in the typically elongated self-assembled QDs which might be useful for the future realization of entangled photon sources.

2. Single and Coupled Pyramidal Cavities

As a promising alternative to conventional pillar-type microcavities, single and coupled pyramidal resonators, partly on top of DBRs, are investigated in A2.8. The latter avoid many of the potential problems of pillars. For instance, QDs can be positioned close to the pyramid tip, which automatically ensures a low number of dots in the cavity. Furthermore, they are fabricated by wet-chemical etching (or self-organized growth on patterned substrates [11]). This avoids the defects typically induced by reactive ion etching or FIB. Indeed, preliminary calculations done in collaboration with the *DFG Research Center MATHEON* [A2.8:15] indicate, that the Q factor in pillar resonators is often not so much limited by surface roughness (as often claimed) but rather background absorption due to a damaged surface layer (see above). The most important advantage of pyramidal cavities, however, is their prospect to enable structures with an improved three-dimensional confinement, leading to high Q factors combined with a potentially low mode volume. This can be achieved by either capping the pyramid facets with Bragg mirrors or by taking advantage of Whispering-Gallery-like modes in free-standing pyramids. Therefore, once optimized, the optical properties of pyramidal photonic structures might be superior to those of pillar cavities.

Fabrication

For the fabrication of our pyramidal resonators we use a technique originally suggested in [12] for a different purpose [A2.8:5,A2.8:9,A2.8:12,13]. It is based on a combination of MBE (in collaboration with A2.6), electron-beam lithography (in the Nanostructure Service Laboratory), and wet-chemical etching involving an AlAs sacrificial layer. A numerical simulation of the process is shown in Fig.8.

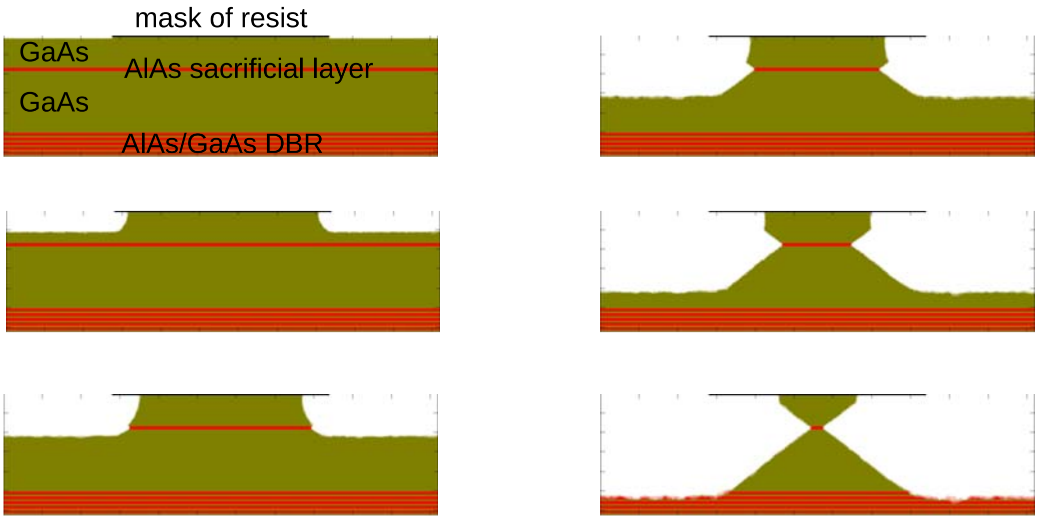

Fig.8: Numerical simulation of the pyramid fabrication process.

MBE is used to grow the initial layer structure which consists of a bottom GaAs / AlAs DBR, the GaAs target layer (~2 µm) for the pyramids (containing the optically active QDs), an AlAs sacrificial layer (~100 nm), and a GaAs cap. Patterning of the sample with square masks by electron-beam lithography (EBL) and subsequent development leaves the substrate covered with resist only at the desired pyramid positions. Afterwards we form the pyramidal structures by etching the sample in a solution based on phosphoric acid, hydrogen peroxide, and water. This etchant is selective and etches the AlAs sacrificial layer at a higher rate than GaAs. In the first step it mainly etches down vertically in the uncovered regions until the sacrificial layer is reached. In the following second step an additional faster lateral etching into the AlAs starts, undercutting the mask from all sides. For a square EBL mask with <100>-oriented sides this initially leads to a square double-pyramid (i.e., a *vertically coupled* double-resonator) with four facets as shown in Fig.9, left.

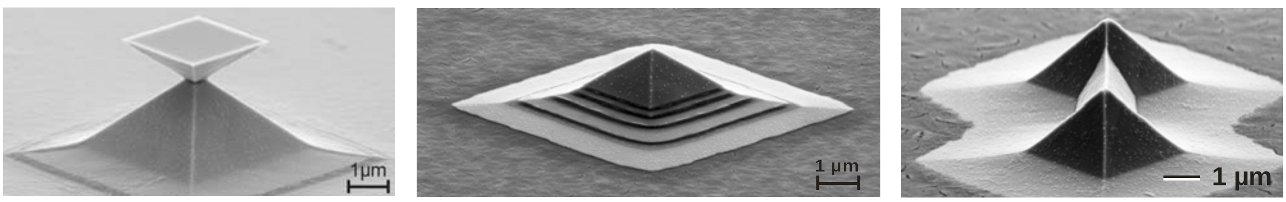

Fig.9: Pyramidal cavities on top of DBRs, fabricated by wet-chemical etching. Left: Vertically coupled double-pyramid. Middle: single pyramidal resonator. Right: Laterally coupled cavities [A2.8:5,A2.8:9,A2.8:12,13].

If the process is continued further, the AlAs is etched through, thus cutting off the upper part and leaving behind a *single* pyramidal resonator on a DBR (Fig.9, middle). Alternatively, the upper part of the structure can be removed using HF (which selectively etches AlAs). In this way, *truncated pyramids* can be realized. Furthermore, more complex structures, in particular *laterally coupled* pyramidal cavities on DBRs (Fig.9, right), can be achieved through utilization of suitable masks. Finally, the facet angle of the pyramids can also be tuned in a wide range by varying the exact composition of the used etchant.

Optical Modes in Pyramidal Cavities

The optical modes of the fabricated pyramidal cavities were measured by µ-PL [A2.8:5,A2.8:9, A2.8:10,A2.8:12,A2.8:17,4,8,13]. An example for the spectra obtained is shown in Fig.10.

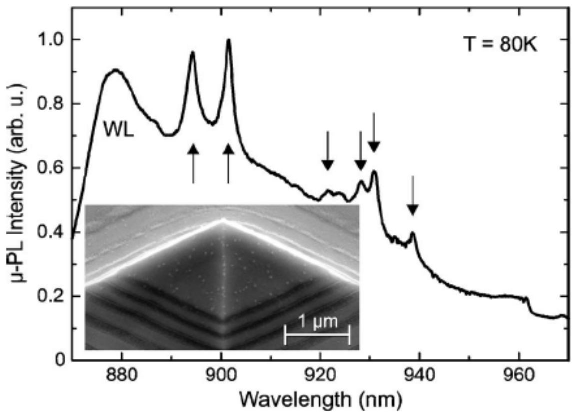

Fig.10: µ-PL spectrum of a single GaAs pyramidal resonator with a base length of 2.4 µm on top of a GaAs / AlAs DBR as shown on the electron microscopic image in the inset. Arrows indicate optical cavity modes, in this case reaching *Q* factors of about 700. WL indicates the wetting layer emission [A2.8:10].

As can be seen, the broad QD emission is clearly modified by the existence of resonant modes in the pyramid structures, proving that the latter act as optical cavities. However, the true nature of specific peaks is only revealed by their temperature dependence, since part of them arise simply from spectral fluctuations in the QD ensemble emission, caused by the statistical size distribution of the dots and their limited number in the small pyramids. These lines shift quite fast to higher wavelengths with increasing temperature due to the quickly decreasing effective band-gap of the dots. On the other hand, peaks related to cavity modes shift at a significantly lower rate, related to the thermal dependence of the GaAs refractive index. Thus, both possibilities can easily be distinguished through temperature-dependent measurements [A2.8:5,A2.8:12]. An example for such an experiment is shown in Fig.11. Several resonant modes with a small average temperature-dependent shift of around 0.06 nm/K are clearly visible, while the QD ensemble and the wetting layer shift at a much higher rate. This value is in good agreement with the expected shift due to the thermal change in refractive index. Therefore, we can confirm that the observed peaks indeed originate from resonant modes in the pyramidal cavity.

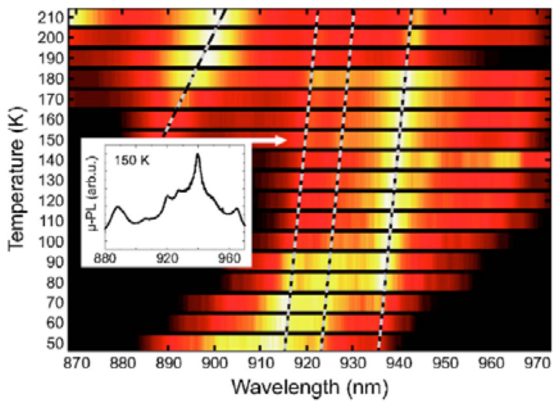

Fig.11: *T*-dependent µ-PL (intensity color-coded) for a pyramidal cavity of 1.9 µm base length and 780 nm height. The inset shows the spectrum at *T* =150 K [A2.8:5].

Finite Difference Time-Domain (FDTD) Simulations

Since the base width of the studied pyramids is often several times bigger than the resonant wavelengths therein, a large density of high-order modes can be expected. Therefore, it was not *a priori* clear, if the observed peaks in our spectra corresponded to *single* modes or groups of the latter. To resolve this issue we utilized the freely available FDTD software package MEEP [14] in order to get a theoretical estimate of the mode structure and expected *Q* factors [A2.8:10,13]. To keep the calculational effort manageable, we had to approximate the actual problem by that of a rotationally symmetric *cone* on top of the DBR.

Figure 12 shows the result of such a calculation for a cone (radius: 1.13 µm, cone angle: 45.5°) sitting on top of a DBR.

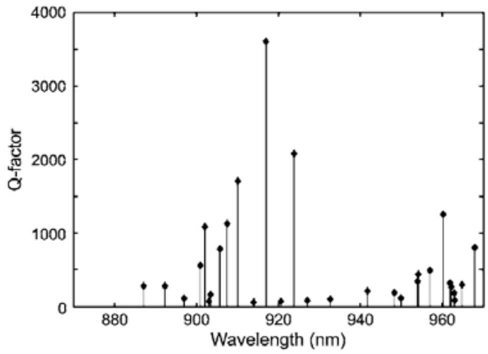

Fig.12: Spectral mode distribution including *Q* factors of a cone (radius: 1.13 µm, cone angle: 45.5°) on top of a DBR according to FDTD results [A2.8:10].

As expected, a high mode density is predicted, however, most modes have very poor *Q* factors. Indeed, the density of modes with fairly high *Q* is comparable with our experiments. The same holds for the *Q* factors themselves (about 700 for the experimentally realized pyramids with non-optimal facet angle). From these results we can conclude that the resonances observed in our spectra generally correspond to *single* modes.

Interestingly, our calculations also show that the achievable Q factor in cone-shaped cavities depends strongly on the cone *angle* [A2.8:10]. A similar dependence would therefore also be expected for pyramidal resonators. Figure 13 (left) shows how the Q factors of the different modes change, when the angle is varied.

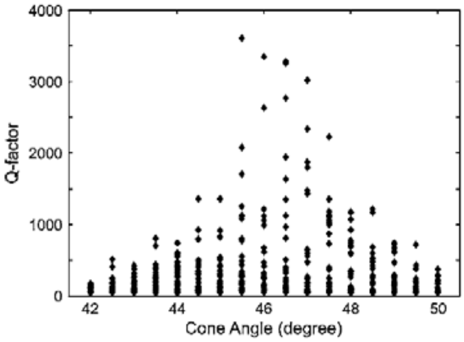

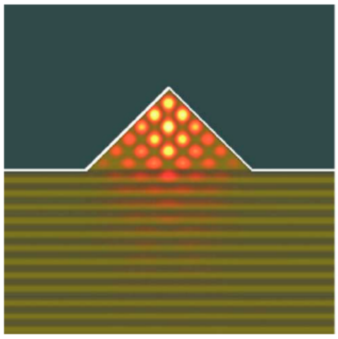

Fig.13: Left: Q factor of different modes in cone-shaped cavities (base radius: 1.13 µm, cone angle varied) on top of a DBR according to our FDTD calculations. Right: Calculated intensity distribution (cross section) for the mode with the highest Q in a resonator with 45° cone angle [A2.8:10].

A sharp maximum for a cone angle of 45.5° is found. This is plausible, because intuitively one would expect the tilted nappe (or pyramid facets) to act similar to a retro-reflector. For the extreme cases of very small or very high angles one could also imagine that "typical" wave vectors of the modes should have relatively steep angles with the surface, resulting in a high transmission through the GaAs–air interface and thus poor optical confinement. The maximum Q is found to be 3600, which is already quite high considering that light confinement at the top of the structure is solely achieved through the refractive index contrast between GaAs and air.

Pyramidal resonators with DBR-Coated Facets

An obvious strategy to improve the Q factor of pyramidal cavities is to coat the top facets with additional Bragg mirrors in order to achieve a strong confinement in all three dimensions. Despite the fact that growth on tilted and pre-patterned surfaces is technologically challenging we have recently succeeded in fabricating high-quality DBR-overgrown cavities based on specially designed truncated pyramidal structures with {114}A facets (see Fig.14) [5].

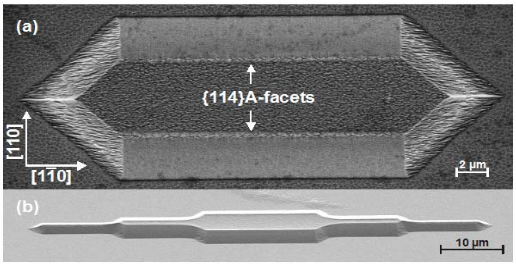

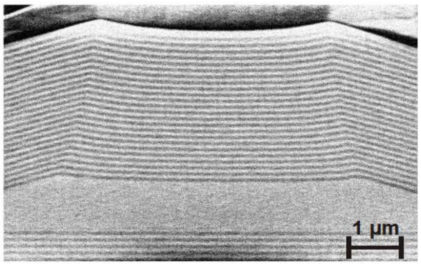

Fig.14: Left: Scanning electron microscopy images of truncated pyramidal structures used for overgrowth. Right: Transmission electron micrograph of truncated pyramid cavity overgrown with AlAs / GaAs DBR [5].

μ-PL measurements of these structures (Fig. 15) revealed that the *Q* factors of such resonators improve by more than an order of magnitude compared to non-overgrown pyramids. Values up to 8000 could be achieved, i.e., in the same range as pillar cavities with similar number of Bragg stacks and mode volume. Furthermore, the broad background observed for uncapped structures (see Fig.10) is strongly quenched, clearly indicating the suppression of poorly confined leaky modes with low *Q*, an important feature for possible future quantum-optical applications.

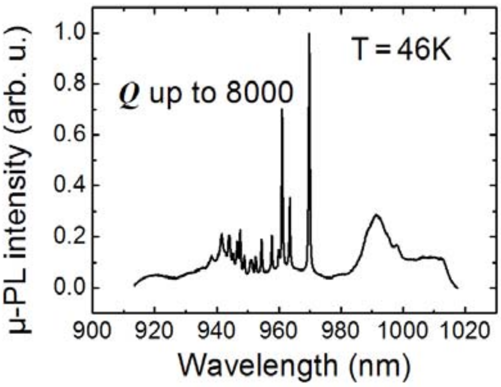

Fig.15: μ-PL spectrum of a DBR-coated pyramidal cavity [5].

Whispering-Gallery-Like Modes in GaAs Cap Pyramids

A promising alternative approach to reach very high *Q* factors in cone-shaped or pyramidal cavities *without any* DBR is to take advantage of strongly confined *Whispering-Gallery-like modes* localized in the *top* part of *double resonators* like the one shown in Fig.16 (left). In preliminary FEM calculations with the *DFG Research Center MATHEON* we found that even in non-optimized structures such modes reach *Q* factors in the order of 10^5 (i.e., equal or superior to the best pillar resonators [9]) while the mode volume can be very low (e.g., the modes do not penetrate into an extended Bragg mirror and are localized at the edge of a relatively small cavity). An example of such a high-*Q* mode is shown in Fig.16 (left). A μ-PL spectrum of Whispering-Gallery-like modes in the top part of a *pyramidal* double cavity is depicted on the right hand side of the same figure. Indeed, sharp peaks due to different modes localized in the upper pyramid are observed (once again confirmed by temperature-dependent measurements, see above). A *Q* factor of ~2700 has already been obtained without any optimization, proving this concept to be very promising.

Interestingly, the spectra shown in Fig.16 could be measured despite the fact, that the optically active QDs were placed in the *bottom* part of the structure. This clearly indicates that the dots can still couple to the Whispering-Gallery-like optical modes, although these are strongly localized in the *upper* pyramid. This aspect could be beneficial for many potential applications, in particular single photon sources, where the light emitted by a single dot has to be efficiently collected and extracted from the photonic structure used. Furthermore, this observation gives direct evidence, that *vertically coupled* cavities based on the double-pyramid design of Fig.9 (left) should be possible.

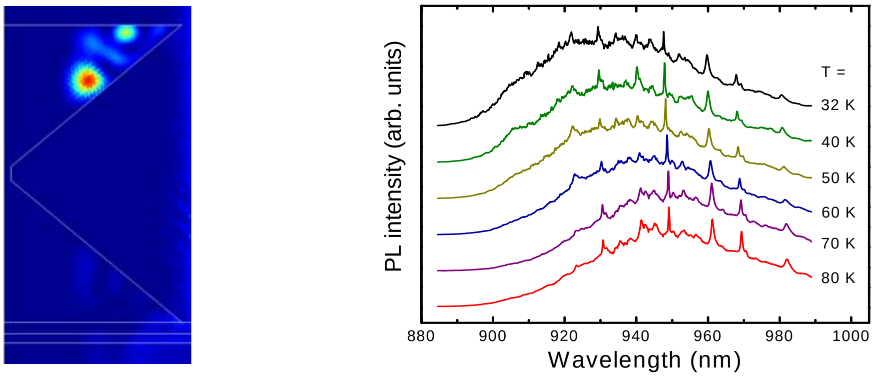

Fig.16: Left: Whispering-Gallery-like mode in the top cone of a coupled double-cone resonator (FEM simulation). Right: Temperature-dependent μ-PL measurements of Whispering-Gallery-like modes localized in the top pyramid of a double cavity similar to that shown in Fig.9 (left). Sharp modes (Q ~ 2700) are observed although the optically active QDs were placed in the *bottom* pyramid. This proves that the dots can still couple to the modes in the upper part of the structure.

3. Single Photon Sources

For quantum-optical applications like single photon sources, cavities that contain only few or even single QDs are often desirable. As already mentioned, one of the main advantages of pyramidal resonators is the fact, that this can be achieved quite easily by incorporating the QD layer close to the pyramid tip. As an example for this approach, Fig.17 shows μ-PL spectra of a vertically coupled pyramidal cavity (similar to Fig.9, left) where the QDs have been incorporated in the top part close to the waist.

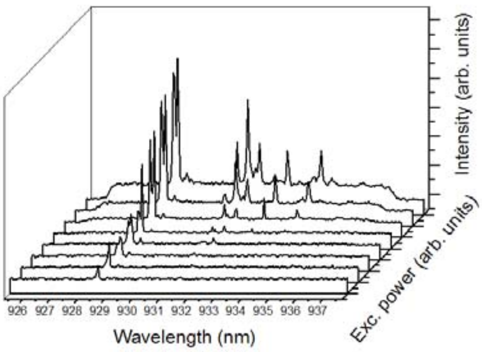

Fig.17: Excitation intensity-dependent μ-PL spectra of few QDs embedded in the top part of a vertically coupled double pyramid (similar to Fig.9, left) close to its waist.

For low excitation powers, only one QD contributes significantly to the spectrum over a wide spectral range. Even for the highest powers, only few lines are visible, part of which are related to excited QD states. This clearly demonstrates that few/single QD cavities can be realized by this approach, thus opening up possibilities for the development of single photon sources based on pyramidal cavities. Since the latter should be operated electrically we have recently started to develop contacted pyramid structures. An example is shown in Fig.18.

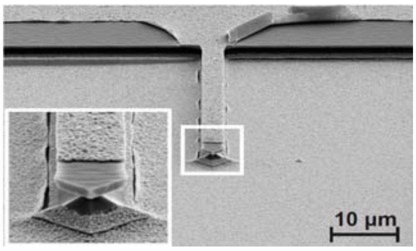

Fig.18: Pyramidal cavity, electrically contacted by a gold layer via a free-standing bridge.

In order to prove single photon emission from these structures we have also realized a Hanbury-Brown & Twiss (HBT) set-up for photon correlation experiments (consisting of a conventional / fiber-based beam splitter and two single photon counters) together with A2.3. The latter will be of key importance not only for the future characterization of pyramidal single photon emitters but also for quantum-optical studies of other resonator types in the next funding period (see below). First measurements of pyramidal structures are currently under way.

The same set-up has also been used to study the feasibility of single-QD spin-injection light-emitting diodes (spin-LEDs, see A2.3) as electrically operated sources for single photons with defined spin. In very recent first measurements we could demonstrate a device with a circular polarization degree (CPD) of 83% for an applied magnetic field B = 2 T and 96% for B = 6 T, respectively. Using 0.5 ns electrical pulses, a strong anti-bunching ($g^{(2)}(0)$ = 0.38) could be observed in HBT photon correlation measurements (see Fig.19). This proves that the spin-LED acts as a source for single photons with the highest polarization degree obtained so far.

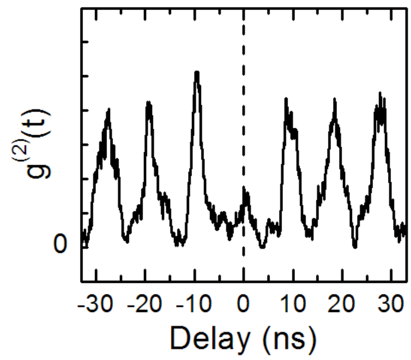

Fig.19: HBT correlation measurement of the photons emitted by a single-QD spin-LED (B = 2 T, T = 5 K) for pulsed (0.5 ns) electrical injection. The strong anti-bunching for zero time delay proves the device to act as a single photon source.

4. Future Perspectives

The outlined activities will be pursued further in the remaining part of the current funding period but shall also be extended to the investigation of high-Q PMMA micro-cone resonators currently studied in A5.4. First experiments to embed suitable core–shell QDs in these cavities and measure their luminescence have already been started. This will lay the foundations for the planned project on cavity quantum-electrodynamics in the next funding period.

References

- own work with complete titles -

[1] A. Imamoğlu, D.D. Awschalom, G. Burkard, D.P. DiVincenzo, D. Loss, M. Sherwin, and A. Small, Phys. Rev. Lett. **83**, 4204 (1999)

[2] J.P. Reithmaier, G. Sęk, A. Löffler, C. Hofmann, S. Kuhn, S. Reitzenstein, L.V. Keldysh, V.D. Kulakovskii, T.L. Reinecke, and A. Forchel, Nature (London) **432**, 197 (2004)

[3] C. Kistner, T. Heindel, C. Schneider, A. Rahimi-Iman, S. Reitzenstein, S. Höfling, and A. Forchel, Optics Express **16**, 15006 (2008)

[4] M. Hetterich, *On a Long Road Towards the Quantum Computer: At the Karlsruhe Center for Functional Nanostructures Tiny Pyramids Made of GaAs Have Been Developed That Might Work as Elements of a Future Quantum Computer* (translated title), interview with Radio Regenbogen, campus report University Radio Baden (Germany), November 13 (2007)

[5] D. Rülke, M. Karl, D.Z. Hu, D.M. Schaadt, H. Kalt, and M. Hetterich, *Optical Microcavities Fabricated by DBR Overgrowth of Pyramidal-Shaped GaAs Mesas*, submitted to J. Crystal Growth

[6] M. Hetterich, **Invited Talk**, *Optical Cavities and Electrical Spin Injection into Single Quantum Dots – Concepts for a Possible Spin-Based Quantum Information Processing*, International School of Atomic and Molecular Spectroscopy, Frontier Developments in Optics and Spectroscopy, Ettore Majorana Center for Scientific Culture, Erice (Italy), 2007, corresponding **Invited Book Chapter** published in summer school proceedings (2008)

[7] M. Karl, S. Li, T. Passow, W. Löffler, E. Müller, D. Gerthsen, H. Kalt, and M. Hetterich, *Optical Modes in Coupled Pillar Microcavities*, Proc. European Conf. on Lasers and Electro-Optics (CLEO Europe), Munich, Germany, 2007, paper CK-2-MON, CK-238.pdf (2007)

[8] M. Hetterich, F.M. Weber, M. Karl, J. Lupaca-Schomber, W. Löffler, S. Li, T. Passow, J. Hawecker, D. Gerthsen, and H. Kalt, **Invited Talk**, *Pyramidal and Pillar-Type Optical Cavities*, Symposium Nano Optics, Konrad-Zuse-Zentrum für Informationstechnik (ZIB), Berlin (Germany), October 19 (2006)

[9] S. Reitzenstein, C. Hofmann, A. Gorbunov, M. Strauß, S.H. Kwon, C. Schneider, A. Löffler, S. Höfling, M. Kamp, and A. Forchel, Appl. Phys. Lett. **90**, 251109 (2007)

[10] M. Bayer, T. Gutbrod, J.P. Reithmaier, A. Forchel, T.L. Reinecke, P.A. Knipp, A.A. Dremin, and V.D. Kulakovskii, Phys. Rev. Lett. **81**, 2582 (1998)

[11] I. Suemune, T. Shimozawa, and K. Hoshi, Physics of Semiconductors, Proc. 26th Int. Conf. Phys. Semicond., Edinburgh (Scotland, UK), 2002, ed. by A.R. Long and J.H. Davies, Conf. Series **171**, Institute of Physics, Bristol, Philadelphia (2003)

[12] V. Cambel, D. Gregušová, and R. Kúdela, J. Appl. Phys. **94**, 4643 (2003)

[13] M. Karl, T. Beck, F.M. Weber, J. Lupaca-Schomber, S. Li, D. Hu, D.M. Schaadt, H. Kalt, and M. Hetterich, *Optical Cavity Modes in Micro-Pyramids*, Conference on Lasers and Electro-Optics (CLEO) / Quantum Electronics and Laser Science (QELS) Conference and Photonics Applications Systems Technologies (PhAST), 2008, San Jose, California, USA, Technical Digest, Optical Society of America, Washington, DC, QFO6.pdf (2008)

[14] A. Farjadpour, D. Roundy, A. Rodriguez, M. Ibanescu, P. Bermel, J.D. Joannopoulos, S.G. Johnson, and G. Burr, Opt. Lett. **31**, 2972 (2006)